Research Article

A Detailed Analysis of Sediment Particle Sizes and Clogging in Permeable Pavements†

Peter W. B. Nichols and Terry Lucke*

University of the Sunshine Coast, Faculty of Science, Health, Education and Engineering, Maroochydore, Australia

Correspondence: Dr. T. Lucke, University of the Sunshine Coast, 90 Sippy Downs Drive, SIPPY DOWNS, QLD 4558, Australia

Email: tlucke@usc.edu.au

Keywords: Clogging, Infiltration, Particle size distribution, Permeable Interlocking Concrete Pavements (PICPs), Water Sensitive Urban Design (WSUD)

Abbreviations: ANOSIM, analysis of similarities; **DRIT**, double-ring infiltrometer test; **LID**, low Impact development; **PCA**, principal component analysis; **PICP**, permeable interlocking concrete pavement; **PRIMER**, Plymouth Routines in Multivariate Ecological Research; **PSD**, particle size distribution; **SIMPER**, similarity percentage; **SRIT,** single-ring infiltrometer test; **SuDS**, sustainable drainage system; **USC**, University of the Sunshine Coast; **WSUD**, Water Sensitive Urban Design

†This article has been accepted for publication and undergone full peer review but has not been through the copyediting, typesetting, pagination and proofreading process, which may lead to differences between this version and the Version of Record. Please cite this article as an 'Accepted Article', doi:[10.1002/clen. 20170078]

Received: 8 February 2017; Revised: 8 February 2017; Accepted: 8 February 2017

Abstract

The trapping of sediments within permeable interlocking concrete pavements (PICPs) during infiltration is a key process that contributes to their pollution removal performance. This process also leads to clogging which decreases infiltration capacity and reduces pollution removal performance. Previous studies have shown clogging to be caused by a number of factors, including the trapping of fine particles, construction techniques, the lack of maintenance, and the mass of the trapped sediments. However, results of these studies have been varied, and the processes governing clogging are not well understood. This field study, undertaken over 12 months, measured the infiltration rates of PICPs that had been in service for a number of years. The study examined sediment extracted from the surface joints of pavements in order to correlate reduced infiltration with sediment particle size distributions (PSDs). Principal component analysis (PCA) was used to compare the differences in infiltration rates and the differences in PSD size class groups between the sites and sub-sites. This study found it was the 251--550 µm particle sizes that explained the most variation at sites with lower measured infiltration rates. A better understanding of sediment PSDs and PICP clogging should help designers to install these systems with more confidence in their long-term infiltration and pollution reduction performance.

1 Introduction

Urbanisation results in increased impervious surface areas including car parking areas, roads, driveways, and rooftops [1--3]. One of the consequences of this is increased stormwater runoff volumes which can result in increased soil erosion and stormwater pollution [4], and increased risk of downstream flooding [5].

In recent years, the management of stormwater in urban areas has become a priority issue for those responsible for planning, construction and maintenance of new and existing developments. The relatively recent initiative of Water Sensitive Urban Design (WSUD) in Australia has highlighted the need for adequate treatment of stormwater runoff from urban developments. WSUD is of a similar design philosophy to low impact development (LID) in the US, and sustainable drainage systems (SuDS) in Europe. WSUD is the integration of urban planning with the management, protection and conservation of the urban water cycle that ensures urban water management is sensitive to natural hydrological and ecological processes.

Using permeable pavements as an alternative to conventional impervious pavement surfaces embraces the principles of WSUD. Permeable pavement systems have been used globally for over two decades as a WSUD point source control device to reduce pollution loads (suspended solids, nutrients and hydrocarbons) and attenuate peak stormwater flows [3, 5]. Permeable pavements have been shown to significantly reduce stormwater runoff volumes, increase infiltration into the soil, and increase evaporation compared to conventionally constructed pavements [5]. They also improve water quality through filtration processes that occur within the pavement structure [6--9]. The majority of stormwater treatment occurs through the removal of suspended solids during infiltration of the stormwater into the pavement bedding structure [10]. The suspended solids are captured in the voids within and between individual paving joints, and in some cases, within the pavement material itself [8]. There have been numerous research studies outlining the combined benefits of permeable pavements in relation to supporting pedestrian and vehicular traffic loads and the control and treatment of stormwater [6, 10--12].

The two main types of permeable pavements are monolithic and modular. Monolithic types include porous concrete and porous asphalt pavements. The majority of modular permeable pavement systems consist of concrete pavers with open joints which allow for infiltration between the pavers and bedding layers. These are generally known as permeable interlocking concrete pavements (PICPs). PICPs are designed to allow infiltration of stormwater through the joints or apertures in the pavement surface. The filtered stormwater then generally either drains through the adjoining soil and into the groundwater table, or is directed into the stormwater drainage system through subsurface pipes included in the PICP structure. A typical PICP pavement is shown in Fig. 1.

The trapping of sediment and other pollutants within the PICP layers during infiltration is an important process that contributes to their pollution removal performance. However, over time, this process can lead to clogging of the PICP surface which results in reduced infiltration capacity, and lower pollution removal performance.

Previous studies have found PICP infiltration rates to be affected by the trapping of fine particles in the upper layer of pavement joints [9, 13, 14]. Baladès et al. [15] explained that as smaller particles trap larger particles, the rate of clogging will increase as more fines are trapped. Other factors thought to influence the clogging process include antecedent dry periods [16], and the total mass of the trapped sediments [11]. Pezzaniti [17] found two levels of sediment accumulation to be critical to PICP performance. The first was that coarser sediment trapped in the relatively small upper horizon of PICPs effectively blocked finer sediment flow to lower filter layers. The second was that the fine sediment that was retained on geotextile layers. Few studies have focused specifically on which portions of the sediment particle size distributions (PSDs) have the most effect on the infiltration performance and clogging of operational field PICP installations.

This study measured the surface infiltration rates of PICP field installations at a total of 52 sites at three different locations. On completion of the infiltration testing, the sediment material trapped between the PICP joints was removed from the paving blocks directly underneath the test location position. PSD analysis was undertaken on the excavated material. Statistical analysis was performed on these results to identify potential correlations between measured infiltration rates and sediment PSDs. The purpose of the study was to determine whether any particular range of sediment sizes were correlated with lower PICP infiltration rates.

2 MATERIALS AND METHODS

The focus of this study was to identify the most influential sediment particle size affecting PICP clogging. Sediment particle size is, however, only one factor among others that potentially affects PICP infiltration rates and clogging. Others include construction materials and methodology, pavement age, and pavement type. In order to differentiate between the effect of PSDs and these other factors on clogging, these elements were incorporated into the experimental design as much as possible.

The study investigated three different PICP installations across the Sunshine Coast in Australia. The three installations were located at Sippy Downs, Cotton Tree and Maleny, and each installation incorporated 23 different construction techniques (Fig. 2, Table 1). Due to the range of different construction techniques used, the Sippy Downs location consisted of six sub-sites at each site. Two replicate infiltration measurements (106 in total) at each sampling site), and 53 sediment samples were taken.

It should be noted that the PICPs evaluated in this study were generally designed and constructed according to relevant Australian guidelines. Other countries may have different construction guidelines and the results of the study may not necessarily be applicable to PICPs in other countries.

2.1 USC PICP Test facility

In 2010, a specially designed 120 m^2 PICP testing facility was constructed in a car parking area at the University of the Sunshine Coast (USC) in Sippy Downs (Fig. 2a and b) to be used as a taxi drop-off and pick-up point for the University. The PICP used for the test facility were Ecotrihex® pavers (Adbri) with a size of 181 mm × 88 mm × 80 mm. These PICPs have apertures and spacing nibs that allow a close fit between pavers while maintaining a suitable joint width. The joints are typically filled with 2--5 mm bedding aggregate. The PICP testing facility comprised six different 20 m^2 test sites (sites 1.1--1.6). Each of the six sites contained six sub-sites, making a total number of 36 test sites at this location. Geofabric liners (Bidim® A19) were installed below the aggregate sub-base at sites 1.3.1--1.3.6 and 1.6.1--1.6.6. Geofabric layers (Bidim® A19) were installed below the aggregate bedding layer at sites 1.1.1--1.1.6, 1.2.1--1.2.6, and 1.3.1--1.3.6.

2.2 Cotton Tree PICP Demonstration Site

The Cotton Tree PICP location (Fig. 2c) was constructed by Sunshine Coast Council in 2008 as a permeable pavement demonstration site (Fig. 2c). The PICP used were Ecotrihex® pavers (Adbri) with a size of 181 mm × 88 mm × 80 mm (sites 2.1--2.11). This location is a suburban roadside carpark area (750 m^2). Sub-base construction details included a sand bedding layer of 50 mm and a geofabric liner (Bidim® A19).

2.3 Maleny PICP Demonstration Site

The Maleny PICP location (Fig. 2d) was constructed by Sunshine Coast Council in 2011 to treat polluted stormwater from a heavy vehicle carpark pavement (0.5 ha) prior to discharge into an adjacent nature reserve. The PICP used were Hydrapave™ (115 mm × 230 mm × 80 mm), supplied by Boral. A permeable sub-base course (minimum of 250 mm) was used during construction. Geofabric liner (Bidim® A19) was installed below the aggregate sub-base.

2.4 PICP infiltration performance expectations

2.4.1 Location 1: Sippy Downs

Infiltration rates measured at the Sippy Downs location were expected to be higher than those found at the other sites due to its relatively recent construction, and lack of stormwater run-on with the potential to carry sediment and cause clogging. In addition, variations in infiltration rates were expected due to the different construction techniques used across these sites. These included the use of a geofabric layer in sites $1.3_{(1\text{-}6)}$, $1.4_{(1\text{-}6)}$ and $1.6_{(1\text{-}6)}$, and the use of a shallow aggregate layer for sites $1.1_{(1\text{-}6)}$ and $1.4_{(1\text{-}6)}$. Lower infiltration rates were also expected at sites 1.1 and 1.4 due to higher sediment loads resulting from greater traffic volumes at these two sites.

2.4.2 Location 2: Cotton Tree

Sediment and organics carried by overland stormwater flow from adjacent landscaping and garden beds adjacent to all sites at this location were expected to be the main causes of clogging, and result in decreased infiltration rates at these sites. All sites experience overland flow run-on from the adjacent road and mixed use recreation area (tennis courts, concrete pavement, and garden beds) catchments. Sand was used as the PICP bedding layer at the Cotton Tree installation and this was unique among the three installations. It was expected that the sand would cause increased PICP clogging and result in lower measured infiltrations rates at sites 2.1--2.11.

2.4.3 Location 3: Maleny

Sites 3.1--3.6 experience overland flow from the adjacent road and an adjacent parkland area comprising mixed species landscaping of turf, shrubs and trees. All sites at the Maleny location appeared visibly clogged and were expected to have relatively low measured surface infiltrations rates.

2.5 SRIT Infiltration Testing

Previous studies on the infiltration capacity of permeable pavements generally used some type of modified single (SRIT) or double-ring infiltrometer test (DRIT) using the falling head method [6, 17--21]. At the time of testing the modified SRIT method was considered to be a commonly used method for measurement of PICP surface infiltration rates. This method was used in this study in accordance with the standard test method for Surface Infiltration Rate of Permeable Unit Pavement Systems ASTM C1781 [22]. The modified SRIT was performed twice in precisely the same location, on each of the test sites. The modification to the SRIT used during testing was the use of a sealant at the base of the ring to prevent horizontal water leakage during testing, ensuring all water that was poured into the ring drained vertically through the pavement structure.

2.6 Particle Size Distribution Analysis

Following the PICP surface infiltration testing, all sediment and materials trapped between and within the joints and apertures from the pavers within the specific area encompassed by ring during the infiltration testing were carefully removed, and collected for laboratory analysis. Material and sediment was separated and categorised using a combination of mechanical separation, and laser diffraction methods. Larger sediment particles (between 150 and 3500 µm) were sorted using mechanical sieves (4, 2, and 1 mm sieves) (ASTM D6913-04) [23]. Sediment sizes <150 µm were analysed using a Malvern Mastersizer 3000™. Bedding material and joint-fill aggregate data was included in the analysis. PSD curves were produced to support visual comparison of sediment sizes between sites. PSD curves were prepared for comparison, while only exemplars have been provided here. Although examination of PSD curves is the conventional method for investigation of soil particle sizes, the similarity of PSD curves observed at different locations with a variety of infiltration rates made additional statistical investigation necessary.

2.7 Statistical Analysis

To compare results between sites, arithmetic means and standard deviations of infiltration rate measurements were calculated for each of the test sites (n = 23). Sub-site analysis was introduced as an additional element to the multivariate analysis because the individual infiltration measurements were specifically taken at the precise locations where sediment sample excavation occurred. Multivariate analyses at the sub-site level (n = 53) were used to identify patterns for groups of particle sizes (Table 2) using Plymouth Routines in Multivariate Ecological Research (PRIMER) [24]. Similarity matrices were calculated using the Bray–Curtis index from non-transformed percentage finer scores for all sites and sub-sites. Analyses of the pairwise comparisons were used to identify any PSD size group differences that occurred between sites and sub-sites and measured infiltration rates.

ANOSIM analysis was used to explain the variation between sites using PSD size class groups and infiltration rates. No transformation and no standardisation of data were required. For interpretation, the Pairwise *R*-values close to zero are indistinguishable, while values closer to 1.0 are separate (all similarities within groups are less than any similarities between groups). Two-way crossed ANOSIM analysis was used to determine whether other factors potentially affected infiltration rate variations. Significant differences are revealed where global *R*-values are >0.75 [24]. Other factors analysed using two-way crossed ANOSIM include: location, inclusion of geofabric layer, presence of geofabric liner, aggregate depth, presence of an impermeable liner, and bedding sand depth.

Principal component analysis (PCA) was performed on the PSD results to compare the differences in infiltration rates and the differences in PSD size class groups between the sites and sub-sites. A PCA can consider either the size class groups or the measured infiltration rates as variables, or both. When PSD size class groups are the considered variables, the analysis creates a set of principal component variables that best explain the variation in measured infiltration rates at the different sites and sub-sites. The extent to which the PCA is a good reflection of the relationship between the samples is summarised by the percent variation explained. Bubble plots were used to represent the relative degree to which the most correlated variable explained the variation in the infiltration rates between sites and sub-sites. The larger the bubble, the greater the amount of variation between sites and sub-sites is explained by that particular size class group relative to the other groups.

Similarity percentage (SIMPER) analysis [24] was undertaken (no standardisation, no transformation, 50% cut-off) to identify which group/s of sediment size classes primarily accounted for the observed variation in categorised infiltration rates (very high > 7000 mm/h; 6999 mm/h < high < 5000 mm/h; 4999 mm/h < medium < 1000 mm/h; low < 999 mm/h). This statistical routine identifies the overall percentage contribution that each PSD size class makes to the average dissimilarity within and between groups. This routine enables identification of a list of PSD size classes ranked in order of importance in discriminating the two sets of related data.

3 Results and discussion

Infiltration rates of the 53 PICP test sites at three locations were found to be between 134 and 13 970 mm/h (Fig. 3). Despite the large variation in measured infiltration rates between (10 300%), and within (0--330%) sites, these results show that at two out of three locations the permeable pavements were still performing satisfactorily within the anticipated designed specifications and able to infiltrate a three month Average Recurrence Interval rainfall event (up to 60 mm/h) [25]. An example PSD curve for three sites with different infiltration rates are shown in Fig. 4.

One-way ANOSIM analysis was performed to determine whether ranked infiltration rates varied showed significant differences between sites. Significant differences are revealed where global *R*-values are greater than

0.5. Cotton Tree and Maleny locations were significantly different from the Sippy Downs location (global *R*: 0.723, $P < 0.001$), but not from each other (pairwise comparison global *R*: 0.426, $P < 0.004$).

PCA found that two variables could describe over 81% of the variation found in measured infiltration rates between sites (Fig. 3). The first principal component explained 68.8% of variation (Table 3). This was caused by negatively weighted size class group variables of 551--1250 and 1251--3500 µm size compared to positively weighted finer particle size class groups of 0--250 µm. A separately weighted 251--550 µm size grouping (0.096) described variation differently. Further PCA investigation into the contributions made by size class groups through bubble plots suggest that the particle size groups 551--3500 µm contributed approximately equally to explaining the variation in infiltration rates greater than 6000 mm/h (Figs. 5 and 6). The separately weighted 251--550 µm size grouping were more associated with explaining the variation in infiltration rates lower than 1000 mm/h (Fig. 7). The remaining size class groups (0--5 through to 151--250 µm) barely featured in explaining the variation between measured infiltration rates at different sites within the first PC (Table 4).

The second PC explained 12.9% of variation and was largely dominated by the equally opposite weighted variables 0--60 and 61--250 µm (Table 4). The PSD size grouping found to explain variable infiltration rates differently in the second PC was the 251--550 µm size grouping (--0.549). The 251--550 µm size group was the group most featured in both PCs, and is shown as a bubble plot in Figure 7 to visually describe the influence of this particle size group and its correlation with lower infiltration rates (Table 4).

SIMPER analysis determined the percentage contribution of each PSD size group to the average similarity within sites, and the average dissimilarity between sites. This gives an indication of which particle sizes are most correlated both within each site and between sites. Average similarity within PSD size class groups (among sites) was high and characterized by the larger particle sized groups (Table 5).

Most sites had a low average dissimilarity (Table 6). Average percentage dissimilarity of PSD size groupings were largest for 151--250, 251--550, 551--1250, and 1251--3500 µm groups (Table 7). There were no PSD size class groups finer than 150 µm that contributed up to the first 50% of variation in infiltration rates between sites. These analyses show that although generally similar to other groups, these larger sized particle size-class groupings were the largest contributors to differences in sites with lower infiltration rates.

Two-way crossed ANOSIM analysis of PSDs performed to determine whether other factors potentially affected infiltration rate variations showed no significant differences (revealed where global *R*-values are greater than 0.5), including: location (global $R = 0.426$; $P = 0.0002$) where the Cotton Tree and Maleny sites were different (but not significantly) from the Sippy Downs site, presence of geofabric layer (global $R = 0.367$; $P = 0.0001$), PICP type (global $R = 0.048$: $P = 0.36$), geofabric liner (global $R = 0.159$; $P = 0.59$), aggregate depth (global R = --0.03; $P = 0.57$), presence of impermeable liner (global $R = 0.159$; $P = 0.67$), and bedding sand depth (global $R = 0.251$; $P = 0.011$).

This field-based study analysed factors affecting clogging of PICPs. The PSDs of the material and sediment trapped in the surface layers and between the pavement joints of PICPs were correlated with corresponding infiltration rates. Differences between PSD curves were difficult to differentiate, based on infiltration rates alone. Similar PSD curves were prepared from sediment collected at sites with very different measured infiltration rates. The close similarity of PSD curves across the range of sites highlights the difficulty of drawing conclusions from this method of data analysis alone.

The infiltration rates measured at the three locations were significantly different. The main difference was between the infiltration rates found at the Sippy Downs location compared with the other two locations. Location, and other factors analyzed in the study were not statistically significant, however, other factors which might explain the difference could be the absence of runon, pavement age, and traffic loading. This may possibly be explained by the absence of stormwater run-on to the Sippy Downs pavement due to its unique design. The pavement was specifically designed to reduce sediment transport onto the pavement area and this should result in less clogging.

PCA analysis found three larger particle size class group variables, 251--550, 551--1250, and 1251--3500 µm explained most of the variation in measured infiltration rates between sites. Both 551--1250 and 1251--3500 µm particle size groups were associated with high infiltration rates. It was the 251--550 µm particle size group most associated with sites with the lowest infiltration rates. This was different to findings of some previous studies [13, 14], the finer particle size class groups (0--5 through to 151--250 µm) barely featured in explaining the variation between measured infiltration rates at different sites. In contrast to a number of previous studies, this study analysed all of the extracted material from the PICP joints and the material was not sieved prior to PSD analysis.

It was not possible to replicate the geofabric layer, bedding sand depth, or geofabric liner construction treatments across all locations. The lack of an orthogonal experimental design may have affected the ability of the statistical tests to fully quantify the influence of the different construction methodologies (geofabric layer, geofabric liner, aggregate depth, PICP type, and bedding sand depth) on infiltration rates found in this study.

As all test sites were genuine field installations, the sediment sampling procedures physically possible excluded extraction of sediment and material from sub-base layers of the pavement. This eliminated extraction of sediment that may have been trapped on the geofabric layer, geofabric liner and impermeable liners across all sites. Conclusions drawn from results found in this study therefore, should only be applied to an understanding of the surface layer clogging processes of PICPs.

The results of the study suggest that it is important for designers to consider the immediate environment surrounding at any proposed PICP location. Surrounding environments that might deliver greater loads of particle sizes between 251--550 µm should be avoided where possible. Where it is not possible, it may be advisable to consider installing pre-treatment measures, such as swales, adjacent to the PICP to reduce the transport of these particles onto the PICP surface. Accelerated PICP clogging may be caused by a range of sediment particle sizes and this may vary from site to site. Appropriate pavement siting in relation to the surrounding environment should ensure longer useful lifespans and potentially reduced maintenance frequency of PICP systems.

4 Conclusions

The focus of this study was to identify factors which were most likely to influence clogging in PICPs, with an emphasis on the examination of sediment particle sizes. The study measured the surface infiltration rates of three PICP field installations. PSD analysis was undertaken on the sediment material trapped on the surface and between the PICP joints. The study found that the relationship between infiltration rates and PSDs of sediment trapped in PICPs is a complex one which is difficult to quantify. For example, this study found that sites with similar sediment PSDs could have very different surface infiltration rates. Using sediment PSD curves alone to infer PICP clogging processes was therefore found to be inadequate. However, the study found it was the 251--

550 μm particle sizes that explained the most variation at sites with lower measured infiltration rates.
While this study provided some interesting preliminary results, it was limited by the range of different PICP field installation sites available for sampling. Examination of a more comprehensive range of PICP field installations, comprising a wider range of construction methodologies, and different site specific environments is planned for future research as this should enable a more thorough analysis to be performed. A thorough understanding of the relationship between sediment PSDs and clogging should help designers of PICPs to specify these systems with more confidence in their long-term infiltration and pollution reduction performance.

Acknowledgements

The project was jointly funded by the Sunshine Coast Council, the University of the Sunshine Coast and the Australian Research Council (Linkage Project Grant-LP120200678). The authors would like to thank Jayden Walter, Dan Layton, Hugh Allan and Bernhard Black from the University of the Sunshine Coast for their assistance during the study.

The authors have declared no conflict of interest.

References

[1] R. J. Carol, Identification and quantification of the hydrological impacts of imperviousness in urban catchments: a review, *J. Environ. Manage.* **2011**, *92*, 1438--1448.

[2] J. Lan, B. Liu, Comparing the Purification effects of sewage water treated by different kinds of porous eco-concrete, in *Proceedings of the 5th International Conference on Bioinformatics and Biomedical Engineering*, ICBBE, Wuhan, China **2011**.

[3] S.-B. Park, M. Tia, An experimental study on the water purification properties of porous concrete, *Cem. Concr. Res.* **2004**, 34, 177--184.

[4] M. J. Bernot, M. Calkins, R.J. Bernot, M. Hunt, The Influence of Different Urban Pavements on Water Chemistry, *Road Mater. Pavement Design* **2011**, *12* (1), 159--176.

[5] J. Sansalone, V. Kuang, X. Ranieri, Permeable Pavement as a Hydraulic and Filtration Interface for Urban Drainage, *J. Irrig. Drain. Eng.* **2008**, 134 (5), 666–674.

[6] C. Dierkes, J. Kuhlmann, J. Kandasamy, G. Angelis, Pollution Retention Capability and Maintenance of Permeable Pavements, in *Proceedings of the 7th International Conference on Urban Drainage*, Portland, OR, USA **2002**.

[7] M. Legret, V. Colandini, C. LeMarc, Effects of a Porous Pavement with Reservoir Structure on the Quality of Runoff Water and Soil, *Sci. Total Environ.* **1996**, 189--190.

[8] M. Legret, M. Nicollet, V. Colandini, G. Raimbault, Simulation of Heavy Metal Pollution from Stormwater Infiltration through a Porous Pavement with Reservoir Structure, *Water Sci. Technol.* **1999**, 39 (2), 119--125.

[9] C. J. Pratt, J. Mantle, P. Schofield, UK research into the performance of permeable pavement, reservoir structures in controlling stormwater discharge quantity and quality, *J. Water Sci. Technol.* **1995**, 32 (1), 63–69.

[10] C. J. Pratt, A. P. Newman, P. C. Bond, Mineral oil bio–degradation within a permeable pavement: Long

term observations, *Water Sci. Technol*. **1999**, 39 (2), 103--109.

[11] T. Lucke, S. Beecham, Field Investigation of Clogging in a Permeable Pavement System, *J. Building Res. Inf.* **2011**, *39* (6), 603–615.

[12] C. F. Yong, A. Deletic, T. D. Fletcher, M. R. Grace, The drying and wetting effects on clogging and pollutant removal through porous pavements, in *7th International Conference on Sustainable Techniques and Strategies in Urban Water Management*, NOVATECH 2010, June 27–July 1, Lyon, France **2010**.

[13] N. Siriwardene, A. Deletic, T. D. Fletcher, Clogging of stormwater gravel infiltration systems and filters: Insights from a laboratory study, *Water Res*. **2007**, 41, 1433–1440.

[14] S. Borgwardt, Long Term In-Situ Infiltration Performance of Permeable Concrete Block Pavement, in *Proceedings of the 8th International Conference on Concrete Block Paving*, San Francisco, USA **2006**.

[15] J. D. Baladès, M. Legret, H. Madiec, Permeable pavements: Pollution management tools, *Water Sci. Technol.* **1995**, 32 (1), 49--56.

[16] E. Fassman, S. Blackbourn, Urban Runoff Mitigation by a Permeable Pavement System over Impermeable Soils, *J. Hydrol. Eng.* **2010**, 15 (6), 475-485.

[17] D. Pezzaniti, S. Beecham, J. Kandasamy, Influence of Clogging on the Effective Life of Permeable Pavements, *J. Water Manage.* **2009**, *162* (2), 76–87.

[18] E. Z. Bean, W. F. Hunt, D. A. Bidelspach, J. E. Smith, Study on the Surface Infiltration Rate of Permeable Pavements, in *Proceedings of the 1st Water and Environment Specialty Conference of the Canadian Society for Civil Engineering*, Saskatchewan, Canada **2004**.

[19] H. Li, J. Harvey, A. Kendall, Field Measurement of Albedo for Different Land Cover Materials and Effects on Thermal Performance, *Build. Environ.* **2013**, 59, 536--546.

[20] E. Z. Bean, W. F. Hunt, D. A. Bidelspach, J. E. Smith, Evaluation of Four Permeable Pavement Sites in Eastern North Carolina for Runoff Reduction and Water Quality Impacts, *J. Irrig. Drain. Eng.* **2007**, 133 (6), 583–592.

[21] C. Gerrits, W. James, Restoration of Infiltration Capacity of Permeable Pavers, in *Proceedings of the 9th International Conference on Urban Drainage*, Portland, OR, USA **2002**.

[22] ASTM Standard C1781/C1781M-14a, 2014, *Standard Test Method for Surface Infiltration Rate of Permeable Unit Pavement Systems*, ASTM International, West Conshohocken, PA, USA **2003**.

[23] ASTM Standard D6913-04, 2004, *Standard Test Method for Particle Size Distribution (Gradation) of Soils Using Sieve Analysis*, ASTM International, West Conshohocken, PA, USA **2003**.

[24] K. R. Clarke, Non-parametric multivariate analyses of changes in community structure, *Austr. J. Ecol.* **1993**, 18, 117--143.

[25] F. Boogard, T. Lucke, S. Beecham, Effect of Age of Permeable Pavements on Their Infiltration Function, *Clean -- Soil Air Water* **2014**, 42 (2), 146--152.

Table 1. Range of different construction techniques used across locations and sites

Location	Site No.	Geofabric layer	Geofabric liner	Aggregate depth (mm)	Impermeable liner	Bedding sand depth (mm)
Sippy Downs	1.1.1--1.1.6	Yes	No	300	Yes	0
Sippy Downs	1.2.1--1.2.6	Yes	No	480	Yes	0
Sippy Downs	1.3.1--1.3.6	Yes	Yes	480	No	0
Sippy Downs	1.4.1--1.4.6	No	No	300	Yes	0
Sippy Downs	1.5.1--1.5.6	No	No	480	Yes	0
Sippy Downs	1.6.1--1.6.6	No	Yes	480	No	0
Cotton Tree	2.1	No	Yes	300	No	>50
Cotton Tree	2.2	No	Yes	300	No	>50
Cotton Tree	2.3	No	Yes	300	No	>50
Cotton Tree	2.4	No	Yes	300	No	>50
Cotton Tree	2.5	No	Yes	300	No	>50
Cotton Tree	2.6	No	Yes	300	No	>50
Cotton Tree	2.7	No	Yes	300	No	>50
Cotton Tree	2.8	No	Yes	300	No	>50
Cotton Tree	2.9	No	Yes	300	No	>50
Cotton Tree	2.10	No	Yes	300	No	>50
Cotton Tree	2.11	No	Yes	300	No	>50
Maleny	3.1	No	Yes	>250	No	0
Maleny	3.2	No	Yes	>250	No	0
Maleny	3.3	No	Yes	>250	No	0
Maleny	3.4	No	Yes	>250	No	0
Maleny	3.5	No	Yes	>250	No	0
Maleny	3.6	No	Yes	>250	No	0

Table 2. Particle size class groups used during multivariate analysis

Particle size class (μm)	Size class
0--5	Fine
6--10	Fine
11--20	Fine
21--40	Fine
41--50	Fine
51--60	Fine
61--70	Fine
71--80	Medium
81--90	Medium
91--100	Medium
101--150	Medium
151--250	Large
251--550	Large
551--1250	Large
1251--3500	Large

Table 3. PCA eigenvalues and variation explained

PC	Eigenvalue	% Variation explained	Cumulative % variation
1	10.32	68.8	68.8
2	1.93	12.9	81.6
3	1.49	9.9	91.5
4	0.75	5.0	96.5
5	0.25	1.7	98.2

Table 4. PCA eigenvector coefficients in the linear combinations of variables

Variable	PC1	PC2
0--5	0.183	0.432
6--10	0.255	0.268
11--20	0.258	0.307
21--40	0.273	0.308
41--50	0.285	0.169
51--60	0.285	0.043
61--70	0.284	--0.048
71--80	0.286	--0.103
81--90	0.290	--0.145
91--100	0.293	--0.170
101--150	0.266	--0.159
151--250	0.216	--0.178
251--550	0.096	--0.549
551--1250	--0.271	0.093
1251--3500	--0.255	0.304

Table 5. Average percentage similarity within groups (among sites)

	Average similarity %	PSD size class group (μm)	Avg. abundance	Cumulative %
Extremely high	71.25	551--1250	30.86	34.56
		251--550	19.63	57.69
Very high	48.26	251--550	17.31	31.54
		151--250	21.70	48.65
High	--	--	--	--
	--	--	--	--
Medium	71.02	251--550	24.24	28.65
		151--250	18.29	48.45
		551--1250	17.01	64.55
Low	--	--	--	--
Very low	--	--	--	--
Extremely low	83.28	251--550	31.16	33.94
		551--1250	20.48	53.38

Table 6. Average dissimilarity between sites

	Extremely high	Very high	High	Medium	Low	Very low	Extremely low
Extremely high	--	37.23	42.24	39.47	55.69	$n < 2$	37.46
Very high	--	--	40.70	39.05	45.10	$n < 2$	39.28
High	--	--	--	19.46	24.25	$n < 2$	18.36
Medium	--	--	--	--	28.48	$n < 2$	22.43
Low	--	--	--	--	--	$n < 2$	27.16
Very low	--	--	--	--	--	--	$n < 2$
Extremely low	--	--	--	--	--	--	--

Table 7. Average percentage dissimilarity of PSD size class groups between sites categorised by ranked infiltration rates. These particle size groups contributed up to 50% of the average dissimilarity between sites. Average abundance is the average importance score.

	Extremely high	Very high	High	Medium	Low	Very low	Extremely low
151--250	8.21	21.70	19.04	18.29	31.70	--	16.01
251--550	19.63		24.22	24.24	0.00	--	31.16
551--1250	30.86	20.08	14.76	17.01	0.00	--	20.48
1251--3500	22.42	15.94	1.00	5.56	0.00	--	2.41

Figure 1. Typical PICP detail

Figure 2. Test locations (a) Sippy Downs after construction; (b) Sippy Downs during construction showing the six separate construction treatments; (c) Cotton Tree; (d) Maleny.

Figure 3. Mean (±SD) PICP infiltration rates at sites. Sites 1.1--1.6: Sippy Downs; sites 2.1--2.11: Cotton Tree; sites 3.1--3.6: Maleny.

Figure 4. PSD curves of sediment found between three exemplar PICP pavement blocks with different infiltration rates (extremely low < 999 mm/h, site 3.1; 4000 < high < 4999, site 1.1; 3000 < medium (M) < 3999, site 2.6). Similar PSD curves were observed at sites with broad ranges of measured infiltration rates.

Figure 5. PCA plot showing the first two PCs responsible for explaining differences in measured infiltration rates. Bubble size describes the extent to which the 551--1250 µm particle size group contributed to the variation explained. Ranked infiltration rates: Extremely low (EL) < 999 mm/h; 1000 < very low (VL) < 1999; 2000 < low (L) < 2999; 3000 < medium (M) < 3999; 4000 < high (H) < 4999; 5000 < very high (VH) < 5999; 6000 < extremely high (EH). Sediment particles sized between 551--1250 µm were more associated with sites with measured infiltration rates >6000 mm/h.

Figure 6. PCA plot showing the first two PCs responsible for explaining differences in measured infiltration rates. Bubble size describes the extent to which the 1251--3500 µm particle size group contributed to the variation explained. Ranked infiltration rates: Extremely low (EL) < 999 mm/h; 1000 < very low (VL) < 1999 mm/h; 2000 < low (L) < 2999 mm/h; 3000 < medium (M) < 3999; 4000 < high (H) < 4999; 5000 < very high (VH) < 5999; 6000 < extremely high (EH). Sediment particles sized between 1251--3500 µm were more

associated with sites with measured infiltration rates >6000 mm/h.

Figure 7. PCA plot showing the first two PCs responsible for explaining differences in measured infiltration rates. Bubble size describes the extent to which the 251--550 μm particle size group contributed to the variation explained. Ranked infiltration rates: Extremely low (EL) < 999 mm/h; 1000 < very low (VL) < 1999; 2000 < low (L) < 2999; 3000 < medium (M) < 3999; 4000 < high (H) < 4999; 5000 < very high (VH) < 5999; 6000 < extremely high (EH). Sediment particles sized between 251--550 μm were generally more associated with sites with measured infiltration rates <1000 mm/h.

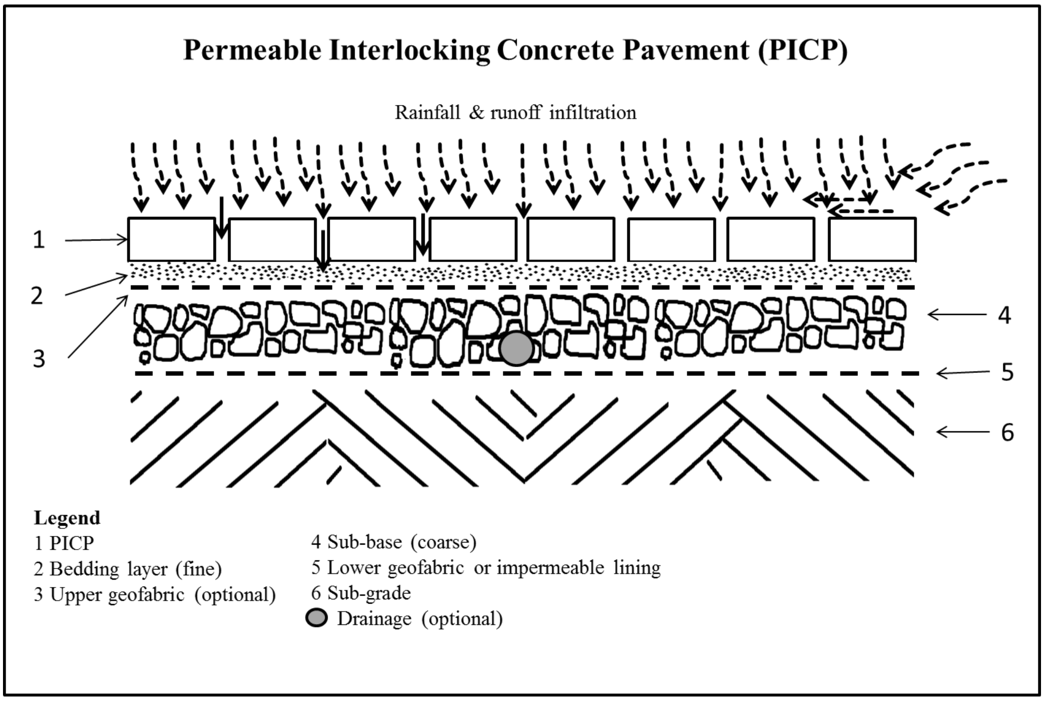

Figure 1

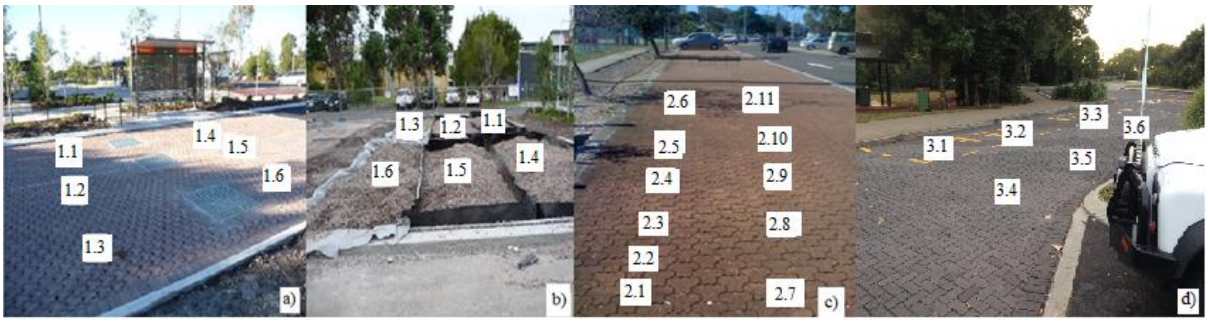

Figure 2

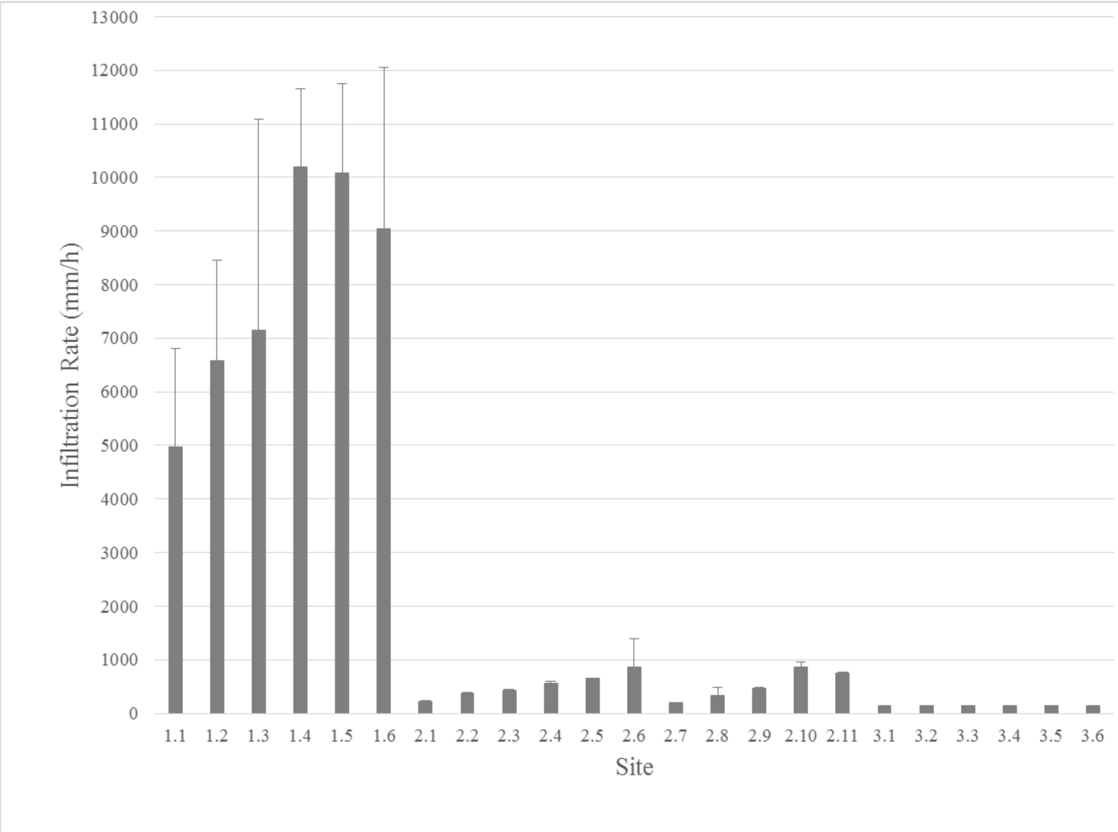

13000
12000
11000
10000
9000
8000
7000
6000
5000
4000
3000
2000
1000
0
Infiltration Rate (mm/h)
1.1 1.2 1.3 1.4 1.5 1.6 2.1 2.2 2.3 2.4 2.5 2.6 2.7 2.8 2.9 2.10 2.11 3.1 3.2 3.3 3.4 3.5 3.6
Site

Figure 3

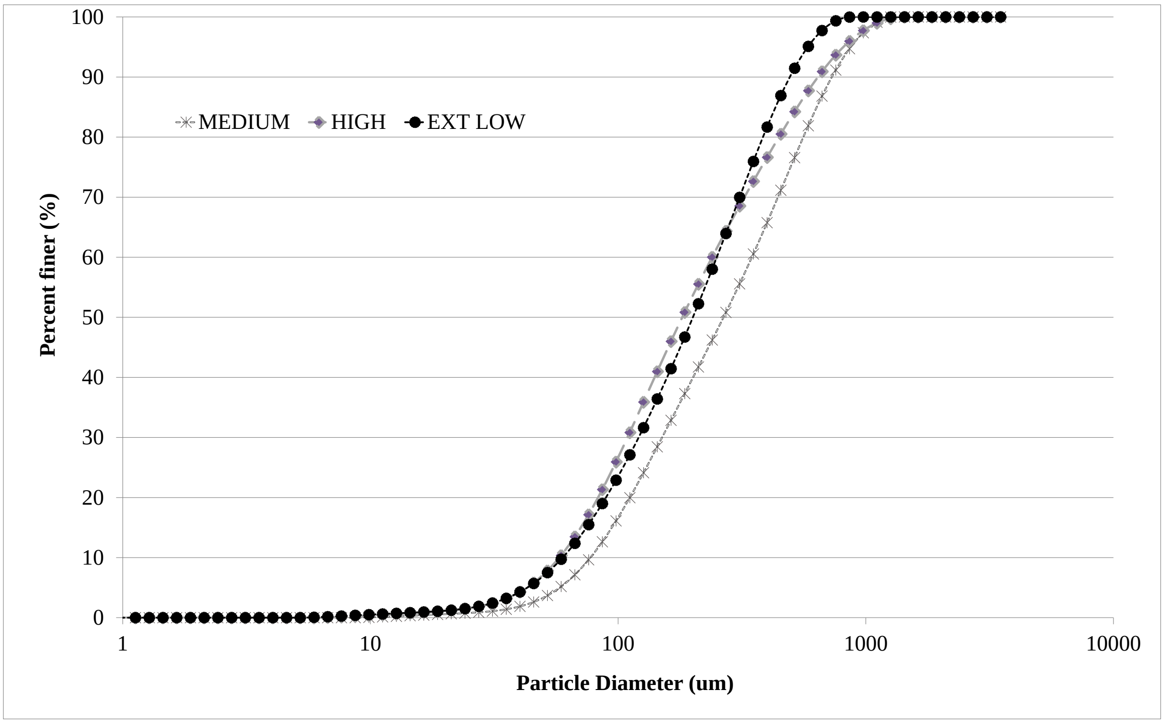

Figure 4

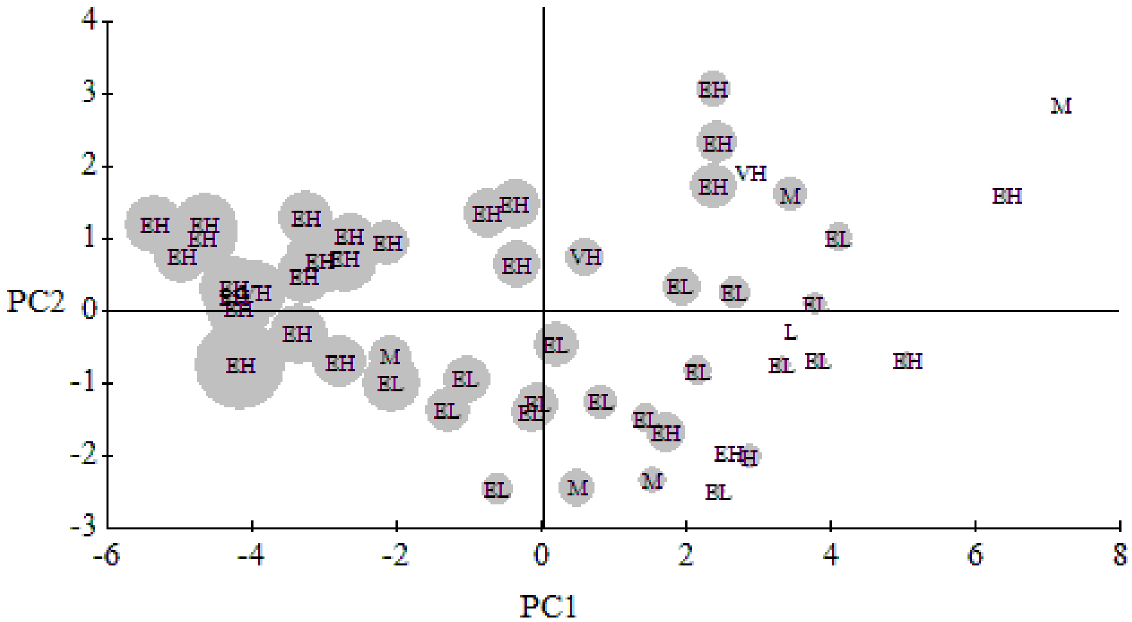

Figure 5

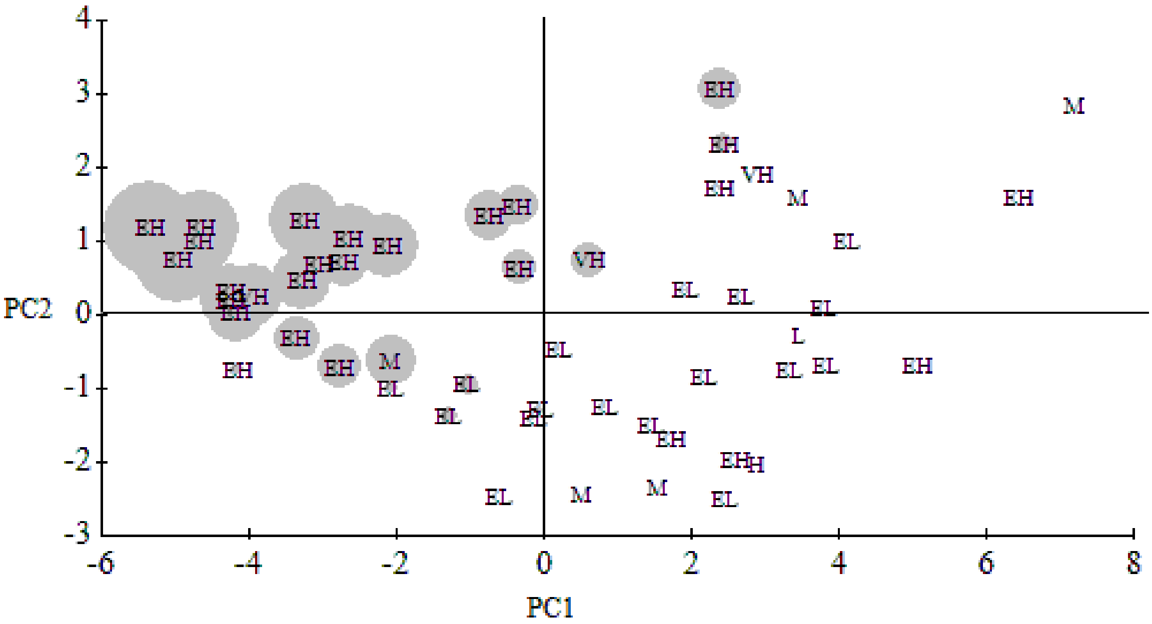

Figure 6

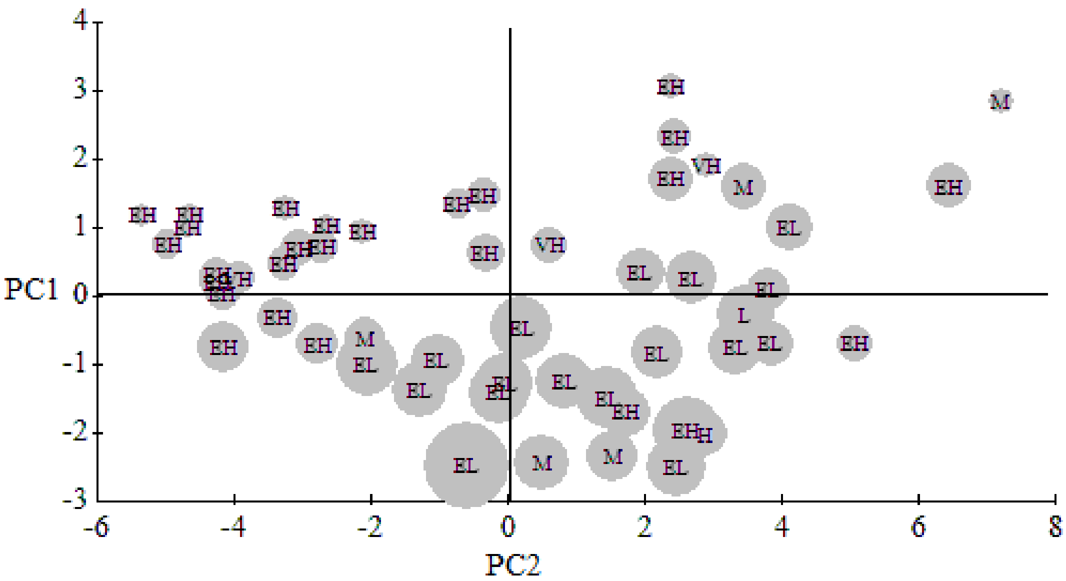

Figure 7